船舶技術研究所報告　第28巻　第3号（平成3年5月）

Plasma sprayed γ - and α -Al_2O_3 coatings.

By

Gillian N. Heintze*
and
Susumu Uematsu*

ABSTRACT

Plasma sprayed coatings generally contain a high proportion of the metastable phase γ-Al_2O_3. This phase has the disadvantage that at high temperatures, above approximately 1200°C, it transforms to α-Al_2O_3 and the structure cracks because of the accompanying density increase. This study has involved determining how to prepare as-sprayed α-Al_2O_3 coatings, their mechanism of formation and a comparison of their structures with as-sprayed γ-Al_2O_3 coatings. Firstly conditions were found where coatings containing greater than 99.5% γ-Al_2O_3 could be prepared, thus ensuring that the injected powder particles, composed of particles of α-Al_2O_3, were completely melted. Then using the same conditions, the torch was traversed slowly over the substrate to produce as-sprayed α-Al_2O_3 coatings. Each pass of the torch produced structures in the coating classified as follows: Type I which contained lamellae of limited length, with lenticular-shaped pores between the lamellae and the lamellae were cracked. It is believed that the impacting particles nucleated as γ-Al_2O_3 and that solidification was complete before the next droplet arrived, but the coating transformed to α-Al_2O_3 on the heat of the torch. Type II, above Type I, where the structure was termed banded-lamellae and the particles were believed to have nucleated directly from the melt as α-Al_2O_3. Solidification was complete before the next droplet arrived to give individual lamellae. Type III, in the upper region of each pass, which consisted of long grains, over 200μm. Grains were believed to have nucleated as α-Al_2O_3 and solidification was not completed before the next droplet arrived. Thermal expansion, thermal diffusivity and pore size distributions were measured, as also were temperatures within the coatings during their deposition.

* Materials and Processing Division

1. INTRODUCTION.

Early workers, when flame-spraying Al_2O_3, noted that their coatings contained predominantly a metastable phase rather than the stable form, α-Al_2O_3[1,2]. The terminology regarding this metastable phase has produced much confusion. It has been referred to as γ-Al_2O_3[1,3,4] and η-Al_2O_3[5,6]. Hurley and Gac[5] based their definition on that of Lippens and de Boer[7] who differentiated between similar patterns of γ- and η-Al_2O_3 by the presence of splitting of the (400) and (004) reflections for γ-Al_2O_3. However, the JCPDS* Powder Diffraction file for γ-Al_2O_3[8], based on the work of Rooksby, does not show any splitting of these lines for γ-Al_2O_3. McPherson[9] after discussion on the metastable phases formed after heating boehmite and bayerite concluded that the structures suggested that γ- and η-Al_2O_3 are closely related to the spinel form and that the observed differences arise from the detailed arrangement of the cation and cationic vacancies. Later, McPherson[10] suggested that strictly the metastable form observed in coatings should be given a new name as the so-called γ-Al_2O_3 structures observed in coatings apparently differ in detail from the γ- and η-Al_2O_3 forms, derived from calcination of aluminium hydroxides. The latter apparently inherit structural features from the original mineral and may also contain residual hydroxyl ions. Since there is no new nomenclature available, that of "γ" will be used here.

Flame and plasma sprayed Al_2O_3 coatings generally contain a few percent of the stable phase α-Al_2O_3 in conjunction with γ-Al_2O_3[3,4,5], where a change in the spraying conditions changes the γ- to α- ratio[11]. Hurley and Gac[5] determined by X-ray diffraction that their coatings contained approximately 15% α-Al_2O_3. Large rounded particles, that had not been properly melted, were evident in coating cross-sections.

α-Al_2O_3 has been quoted as having both superior physical and mechanical properties to γ-Al_2O_3. Since γ-Al_2O_3 is the predominant phase in as-sprayed coatings, efforts have been made to transform this structure to the α- phase by heat treatment. Heat treatments around 900°C to 1000°C produced either no crystallographic change[1] or transformation to δ-Al_2O_3[3,5,10]. It was only after heating above 1260°C for selected periods of time that the transformation to α-Al_2O_3 was complete[1,2,4]. Ault[1] found that the total porosity of the coating increased from 7.6% to 14.6% on heating at 1460°C, even though the sample shrank 0.6%. The apparent paradox occurs because the true density increases from 3.60 g cm^{-3} for γ-Al_2O_3 to 3.98 g cm^{-3} for α-Al_2O_3. The volume shrinkage accompanying the phase transition was also accommodated by "fragmentation" of the structure[5], although holding at 1350°C for a prolonged period resulted in overall densification by sintering. The inherent feature of as-sprayed coatings, ie its lamellar structure,

* Joint Committee on Powder Diffraction Standards

disappeared after heating above 1149°C [4]. Porosity peaked around 1300°C, a three-fold increase on the as-sprayed state and thereafter slowly decreased. The average pore diameter continued to grow with increasing temperature even though the structure was completely α-Al_2O_3. This means that any transformation by heat treatment causes cracking in the structure which is likely to be detrimental to the coatings' mechanical properties.

Production of α-Al_2O_3 as-sprayed coatings seems to be desirable. McPherson[9,12] has made a detailed study on the nucleation mechanisms of flame and plasma sprayed Al_2O_3 coatings. He proposed that during normal circumstances, where the substrate is air-cooled during coating deposition, each droplet experiences considerable undercooling after impact and spreading on the substrate surface ($\sim$0.2Tm**) and, if it is completely melted in the heat source, it will nucleate as γ-Al_2O_3 rather than α-Al_2O_3 because the γ-phase has a lower barrier to nucleation from the liquid than α-Al_2O_3. Then the subsequent thermal history of the droplet determines what phase or phases will be formed; ie γ-, δ-, θ- or α-Al_2O_3. If the rate of crystal growth from the liquid is faster than the rate of solidification to the stable phase, and the cooling rate after solidification is sufficiently rapid to suppress subsequent transformation, γ-Al_2O_3 will be retained to room temperature[12]. These conditions are typical for plasma sprayed Al_2O_3 where usually a strong blast of cooling air is used. Lamellar thickness must also be considered[9]. Estimated time-temperature relationships for Al_2O_3 suggested that the transformation to α-Al_2O_3 during crystallisation would become significant at lamellae thickness greater than approximately 20μm for cold substrates, and thicknesses greater than 10μm for substrates at temperatures greater than 1000°C. Furthurmore, if there is an unmelted part of the seed nucleus, this acts to nucleate the α-phase, as in most cases the original powder is α-Al_2O_3. This explains the low levels of α-Al_2O_3 in the coatings and this level increases as either the power of the torch is decreased or the powder particle size is increased[9].

Thus a hot substrate is essential in order to produce α-Al_2O_3 coatings directly by plasma or flame spraying. Little work appears to have been published in this area. Huffadine and Thomas[13] determined that the temperature of both the substrate and the sprayed coating should be above the $\gamma \rightarrow \alpha$ transformation temperature. Their experimental evidence indicated that cooling below 1000°C must be avoided or else the already deposited material cracked. This extra heat was supplied by a furnace into which the spirally sprayed part was gradually inserted as spraying proceeded. The subsequent furnace cooling rate was 70°C h^{-1}. Dense components, with an open porosity of 3.9% could be fabricated when ambient temperatures were in excess of 1400°C.

** Melting Point

Fielder[14] brought the torch closer to the substrate, thereby increasing the temperature of the latter and so producing deposits of α-Al_2O_3. Optical microscope observations revealed that the coating had an abrupt change in microstructural morphology about midway through the thickness of the sample. In one half, there was a fragmented structure of α-Al_2O_3 believed to result from the transformation of γ-Al_2O_3, and in the other half a columnar structure, also α-phase, believed to form directly from the melt. Fielder postulated that possibly the temperatures were in excess of 1400°C.

In this work, a more detailed study of as-sprayed α-Al_2O_3 coatings is made and their structures are compared with those of γ-Al_2O_3 containing coatings. Firstly, coatings containing greater than 99.5% γ-Al_2O_3 were produced, thus ensuring that there was little likelihood of a seed nucleus of α-Al_2O_3. Then using the same torch conditions and the same torch-to-substrate distance, but slowly traversing the torch over the substrate with little or no air cooling to ensure slower solidification and cooling conditions, dense Al_2O_3 coatings of small size were fabricated. Substrate and coating temperatures were monitored. The structures and mechanisms of formation of both coating types are discussed.

2. EXPERIMENTAL METHOD AND RESULTS.

2.1 Production of optimum γ-Al_2O_3 containing coatings.

Coatings were sprayed in air with a 40kW subsonic Plasmadyne SG-100 plasma torch, with backward powder injection, onto grit blasted mild steel substrates of dimensions 60mm x 60mm x 2mm. Up to six substrates could be simultaneously mounted on a rotating holder which had internal air cooling via a coiled pipe containing many holes, Fig. 1. X-ray diffraction of the Al_2O_3 starting powder, Showa Denko K16T, with particle diameter range 10-40μm, showed that it contained ~96% α-Al_2O_3 and ~4% β-Al_2O_3. By systematically varying the torch power and the torch-to-substrate distance, conditions were found where coatings containing >99.5% γ-Al_2O_3 could be produced. Torch parameters for these optimised parameters, including the necessary cooling conditions are given in Table I.

2.2 X-ray diffraction of γ-Al_2O_3 coatings

X-ray diffraction spectra (Phillips Automated Powder Diffraction unit, 40 kV, 40 mA, 0.5 deg min^{-1}, $K\alpha_2$ subtracted) of an optimised γ-Al_2O_3 coating is given in Fig. 2 where the torch-to-substrate distance was 9 cm. Given this optimised power level of 33kW, and successively decreasing the torch-to-substrate distance in ~2 cm steps, from 11cm to 5cm, it is seen that as this distance decreased, the γ (400) peak gradually broadened and split, Fig. 3, and the level of α-Al_2O_3 increased. Minor broadening of the γ (400)

Table I. Spraying conditions for optimised γ-Al_2O_3 coatings.

Arc current (A):	950
Arc voltage (V):	34~35
Arc gas (ℓ min^{-1})	
Argon (primary) at 0.34 MPa	47
He + 10%H_2 (secondary) at 0.21 MPa	8.5
Powder carrier gas (Argon, ℓ min^{-1}) at 0.19 MPa	4.7
Powder feed rate (g min^{-1})	10.6
Torch-to-substrate distance (cm)	9.0
Coating thickness (mm)	1< t < 2
Holder rotation speed (rev min^{-1})	23
Torch traversing speed (cm min^{-1})	20 to 31
Cooling air pressure (MPa)	0.44

peak was also observed from coating surfaces that had been in contact with the substrate and subsequently forcefully removed.

X-ray diffraction spectra after heat-treatment of as-sprayed optimised γ-Al_2O_3 free standing pieces placed in a pre-heated furnace for selected times and temperatures, Fig. 4, showed that splitting of the γ (400) peak rapidly occurred between 700 and 800°C to produce δ-Al_2O_3[15], although the intensities did not have corresponding ratios with that of the JCPDS spectra. The nomenclature, δ'', was defined here to describe the intermediate tetragonal phase between the cubic γ-phase and the JCPDS tetragonal δ-phase. After a longer heating time, the δ-Al_2O_3 coating transformed to α- and θ-Al_2O_3, and finally was fully converted to α-Al_2O_3.

2.3. Microstructures of γ-Al_2O_3 coatings.

Top and fracture faces of as-sprayed γ-Al_2O_3 coatings are presented in Fig. 5. Each droplet had spread out on impact to form a splat and fine cracks appeared within each splat. Lamellae were typically 1 to 4 μm thick and contained grains of order 0.1 to 1 μm in diameter.

2.4. Production of as-sprayed α-Al_2O_3 coatings and X-ray diffraction assessment.

Coatings containing more than 2 to 3 % α-Al_2O_3 could not be produced by spraying onto the rapidly rotating sample holder (up to 80 rev min^{-1}) using the optimised spraying parameters for γ-Al_2O_3, even if there was no cooling air. It was determined that much higher temperatures and slower cooling rates within the coating were required to produce α-Al_2O_3 coatings and this could possibly be achieved by continuously keeping the heat of the torch on only one substrate and slowly traversing the torch across that

substrate. Since the substrate was mild steel, ZrO_2-Y_2O_3 was selected to be applied as a coating both to promote slower cooling of the Al_2O_3 coating and to reduce oxidation of the substrate. Spraying parameters for the ZrO_2-Y_2O_3 coating were of either one of two conditions and are given in Table II. In both cases the resultant coating had a non-transformable tetragonal crystal structure. Al_2O_3 was then sprayed onto one of these ZrO_2-Y_2O_3 coatings, using the previously determined torch parameters and torch-to-substrate distance to spray optimised γ-Al_2O_3 coatings, but the substrate was held stationary and the torch traversed over the substrate.

Initially the cooling air pressure was set at 0.15 MPa and the torch was traversed backwards and forwards at 31 cm min^{-1} over a distance of approximately 50 to 55 mm, Fig. 6(a). This produced a thick coating that remained red hot in colour for several seconds after the torch was traversed off the coating and extinguished. The coating had steep sides, which formed a ridge subtending an angle of approximately 90°, Fig. 6(b). A polished face from the central region of the coating contained only α-Al_2O_3, Fig. 6(c), however the steep sides of the outer surface contained δ'' -Al_2O_3 in addition to α-Al_2O_3, Fig. 6(d). Reducing the air pressure to 0.03 MPa reduced the ratio of the δ'' - phase to α-Al_2O_3, however reducing the travelling speed to 20 cm min^{-1} made no difference to this ratio. For these thick coatings of order 10mm, combinations of reducing the cooling air to zero, pre-heating the ZrO_2-Y_2O_3 coating and post-heating the Al_2O_3 coating with the torch, made no reduction to the amount of δ'' - phase on the surface. Given the selected optimised settings for production of as-sprayed α-Al_2O_3 coatings, Table II, it was observed that if coatings were thinner, ie of the order of 4mm thick, and were therefore gently rounded rather than peaked on top, just detectable levels of δ'' -Al_2O_3 were present on the top surface. Further down the sides, the levels of δ'' -Al_2O_3 increased. The Al_2O_3 coating face in contact with the ZrO_2-Y_2O_3 also contained some δ'' -Al_2O_3, but the bottom of the next layer up, on coatings where this layer could be forcefully separated, contained only minor levels of the δ'' -phase.

2.5 Microstructures of α-Al_2O_3 coatings.

In the area of the top ridge of the thick coatings, of thickness of order 10mm as prepared in Table II, droplets spread very well after impact to form smooth discs, Fig. 7(a), which contained networks of fine cracks. Very little splashing due to droplet breakup occurred. Furthur down the sides of the top surface ridge, where the particles did not impact at right angles to the surface, the droplets had spread but also splashed asymetrically to occassionally produce a "wet paint drips" morphology, Fig. 7(b).

The fracture faces were very different to those of as-sprayed γ-

Table II. Conditions for production of as-sprayed α-Al_2O_3 coatings

ZrO_2-$8Y_2O_3$ undercoat: Either one of two conditions	
1: Usual coatings	
Conditions as in Table I excepting	
Powder feed rate (g min^{-1})	14
Torch-to-substrate distance (cm)	10
Coating thickness (mm)	0.6 to 1.3
2: For temperature measurements (Sec. 2.7)	
Conditions as above, and Table I excepting	
Stationary mild steel substrate	
Cooling air (MPa)	0.44
Torch traversing speed (cm min^{-1})	20
As-sprayed α-Al_2O_3 coating: torch conditions as in Table I excepting	
Stationary ZrO_2-Y_2O_3 coated, mild steel substrate	
Cooling air (MPa)	0 to 0.03
Torch traversing speed (cm min^{-1})	20
Traversing length (mm)	~50
Coating thickness (mm)	5 to 10
	18 passes = ~10mm

Powder ZrO_2-8wt% Y_2O_3: Showa Denko K90. Particle diameter range: 10-40μm.

Al_2O_3. To the naked eye, a series of horizontal bands, one formed on each pass of the torch, could be clearly delineated, Fig. 7(c). Each pass had a varied microstructure that could be classified into three regions, each of which was repeated in each subsequent pass.

In the first and lower region of any pass, grains up to approximately 4μm in diameter extended the width of the lamellae which was up to 10μm. The lamellae had very limited lateral continuity, Fig. 7(d). Lenticular shaped pores were located between the lamellae and this was referred to as Microstucture Type I. The bottom face of any pass that could be forcefully separated from its neighbour contained larger cracks than those seen on the top surface.

Above this region, in the second region, the grains became progressively longer and wider and the lamellar structure, and its associated lenticular-shaped pores, disappeared, as indicated by an "A" in Fig. 7(e). In

this region, there were also adjacent areas where horizontal "lamellae-bands" were present, indicated by a "B" in Fig. 7(e) and called Microstructure Type II. A higher magnification of this latter type of microstructure is given in Fig. 7(f).

In the upper region of each pass, the third region, the grain's length and width had extended in some passes to over 200μm and 10μm respectively, Microstructure Type III, Fig. 7(g). Occassionally one or several grains abruptly terminated in this region (arrowed) with elongated pores present at some of these termination points. The columnar grains were always wrinkled and occassionally, probably through lack of liquid during solidification, the shape of the columnar grain tips, classified as cellular dendritic[15], could be delineated, Fig. 7(h).

The ratios of these three regions to each other depended on the pass number and where the region of interest was located. For any given pass the proportion of Type III structure started to decrease after moving approximately one quarter the deposit width from the centreline. Right at the edge of the coating, there were no grains of Type III microstructure. At a point midway from the two ends of the traverse, the ratio of Type III to Type I and II (grouped together) progressively increased ranging from approximately 1:1 in the first pass to 3.5:1 for the top pass, number 18. However, to one side of this midpoint, the time for the torch to return was not constant, because of the shorter distance from one end than the other, so a pass with a short return had a larger ratio than the next deposited one, because the latter had a longer return time. When comparing every second pass, however the ratios continued to increase in the direction of the top of the coating.

In some deposits, there were very clear boundaries between each pass, so that the long grains abruptly terminated into the short grained region of the next pass. The passes were usually well joined but occassionally separated by a crack.

If the torch-to-substrate distance was reduced to approximately 8.5cm by continuing to spray, and thus making a very thick coating, the coating deposited at either end of each traverse, where the torch was temporarily stationary for 1～2 seconds, became superheated, Fig. 8(a). When cooled to room temperature, these upper regions had a glassy-like appearance, being somewhat transparent. These glassy regions contained alternating regions of short and long grains but the microstructure of these layers was somewhat different to those presented in Fig. 7. In the area where the grains were short, of order 3 to 15 μm in length and width 1 to 3μm, there was little sign of the lamellae-type structure, Fig. 8(b). These grains appeared somewhat segmented and cracking was obvious. In the region containing the long grains,

the grains were very long up to 500μm in length and up to 80 μm in width, Fig. 8(c). The ratio of the width of the region containing short grains to that containing long grains was approximately 1:3. Porosity, that appeared as numerous small pores up to 1μm in diameter, seemed to preferentially occur in lines lying at right angles to the direction of grain growth. It appeared that the long grains extended from the short grains which were favourably oriented for crystal growth.

When ZrO_2-Y_2O_3 was sprayed at the same slow traversal rate, no regions containing long grains were observed.

2.6. Heat treatment by the plasma torch of as-sprayed γ-Al_2O_3 coatings.

Heating an optimally deposited γ-Al_2O_3 coating with the plasma torch operating as given in Table III made the coating red in colour and produced severe cracking within the top splats, Fig. 9(a), and between the lamellae, Fig. 9(b). The coatings completely transformed to α-Al_2O_3, with the exception of a thin layer that had been in contact with the substrate and contained δ- and α-Al_2O_3.

Table III. Torch conditions for heat treatment of γ-Al_2O_3 coatings.

Arc current (A):	920 or 940
Arc voltage (V):	36
Arc gas (ℓ min^{-1})	
Argon (primary) at 0.34 MPa	47
Helium (secondary) at 0.27 MPa	10.5
No powder feed	
Torch and substrate stationary	
No air cooling	
Torch-to-substrate distance (mm)	72
Heating time (min)	5

2.7 Temperature measurements.

Temperatures both at the substrate surface and within the γ- and α-Al_2O_3 coatings were monitored using Pt-13%Rh thermocouples. The thermocouples were inserted from behind the substrate, through thin Al_2O_3 tubes that had been glued into position using a paste of Al_2O_3 powder and water (Aron Ceramic D). These were either left to dry in the air or rapidly dried with a hand-held hot-air gun.

For the γ-Al_2O_3 coatings, the junction of one thermocouple was spot welded to the grit-blasted substrate surface and the junction of the other placed beside it, but about 0.5 mm above the surface of the substrate.

Both thermocouple junctions were lightly grit-blasted. Since the substrate could not be rotated, as that would cause the thermocouple wires to coil around the rotating holder's shaft, the frequency of torch rotation was simulated by hand spraying. The substrate was still bolted to the non-rotating holder, to maintain the same forced-air cooling conditions. Torch traversal speed, pass frequency and torch-to-substrate distance, as given in Table I, could be reasonably reproduced.

Temperatures within the γ-Al_2O_3 coating during deposition ranged between 400 and 600°C, with substrate temperatures being correspondingly up to 50°C cooler. The temperature range progressively decreased as spraying progressed, but the mean temperature remained approximately the same, Fig. 10(a).

Temperature measurements of the α-Al_2O_3 coatings firstly involved spot welding one thermocouple to the steel substrate surface. Two extra Al_2O_3 tubes plugged with Al_2O_3 paste, projecting approximately 2 mm above the grit blasted face of the substrate, were installed adjacent to the thermocouple. The assembly was then sprayed with ZrO_2-$8Y_2O_3$ as given in Table II. Then the two extra tubes were unblocked and the second thermocouple was threaded through them with its junction placed approximately 0.5mm above the surface of the ZrO_2-Y_2O_3 coating, and a little to the side of the lower already coated thermocouple. The whole was sprayed in the manner required to produce α-Al_2O_3 coatings and temperature profiles recorded from within the ZrO_2-Y_2O_3 and α-Al_2O_3 coatings are given in Fig. 10(b).

2.8 Porosimetry

Porosimetry measurements were made using a Micromeritics Poresizer, model 9310. After each increase in pressure, there was a pause-time of 30 seconds to allow the porosimeter to come near equilibrium. The α-Al_2O_3 sample included several passes and was taken from the central part of the coating. Pore diameter as a function of cumulative intrusion is presented in Fig. 11. The majority of pores fell within 0.07-0.2μm diameter for the γ-Al_2O_3 coatings, with a rapid cumulative volume increase around 0.1μm pore diameter, and within 0.03-0.3μm for the α-Al_2O_3 coatings. Open porosities of the γ-Al_2O_3 and α-Al_2O_3 coatings were calculated to be 6.4% and 4.4% respectively which corresponded to an apparent density of 3.62 and 3.90 g cm^{-3} respectively. Given the absolute density as 3.6 g cm^{-3} for γ-Al_2O_3 and 4.0 g cm^{-3} for α-Al_2O_3, the closed porosity was calculated to be 0% and 1.3% respectively, to give total porosities of 6.4 % and 5.7% respectively.

2.9 Thermal expansion.

Thermal expansion, in an argon atmosphere to 1300°C at a heating rate of 5°C min^{-1} and back to room temperature at the same rate, was measured

by a Shinku-Riko vertical dilatometer, model DL-7000RH, both along the plane of each as-sprayed coating type and at right angles to it. Curves are presented in Fig. 12.

Rapid shrinkage occurred in the γ-Al_2O_3 coatings above 1130°C, with an overall shrinkage after cooling to room temperature of 1.6% in the plane of the coating and 2.7% in the direction at right angles to the coating plane, Fig. 12(a). The expansion rate at right angles to the plane of the coating was approximately 3 times that of the expansion along the plane of the coating, on both heating and cooling. X-ray diffraction after dilatometry showed that the coating had converted completely to α-Al_2O_3. The degree of cracking and the grain size was similar to that of the coatings that had been heat treated by the torch.

The α-Al_2O_3 coatings had negligable shrinkage after the thermal cycle imposed by the dilatometer, Fig. 12(b). Their rate of expansion on heating was approximately that along the plane of the γ-Al_2O_3 coating. In both directions, the α-Al_2O_3 coatings displayed thermal expansion hysteresis, with that in the direction perpendicular to the plane of the coating being quite pronounced.

Thermal expansion to 1300°C at 5°C min^{-1} in an argon atmosphere was also carried out in both directions on as-sprayed γ-Al_2O_3 coatings that had subsequently been heat treated with the plasma torch (Sec. 2.6) and converted to α-Al_2O_3. Shrinkage started around 1100°C in both directions, but it was considerably less than that in the as-sprayed γ-Al_2O_3 coatings, Fig. 13.

2.10 Thermal diffusivity

Mild steel discs of diameter slightly larger than 10mm were glued onto grit-blasted substrates with Aron Ceramic D. Discs to be sprayed to produce γ-Al_2O_3 were placed over 8mm diameter holes in the substrate, so that the cooling air could directly impinge on their back surface.

Thermal diffusivity measurements were carried out with the as-sprayed γ-Al_2O_3 coating adhering to the mild steel disc; the thermal diffusivity of the latter having been previously measured. The as-sprayed α-Al_2O_3 coatings on the otherhand were free standing, since the ZrO_2-Y_2O_3 coating conveniently separated from the disc after spraying and this latter coating was subsequently removed by filing with a diamond file. γ-Al_2O_3 coatings converted to α-Al_2O_3 by heat treatment with the torch (Sec. 2.6) were also included, where the coating detached from the substrate during the heat treatment. All coatings were given a light coating of carbon prior to measuring their thermal diffusivity at room temperature using a Shinku-Riko model TC-7000 recorder. Measured thermal diffusivity values and subsequently calculated thermal conductivity values are tabulated in Table IV.

Table IV. Thermal Diffusivity Data

Coating	Thickness (mm)	Thermal Diffusivity ($cm^2\ s^{-1}$)	Density ($g\ cm^{-3}$)	Thermal Conductivity[1] ($W\ m^{-1}\ K^{-1}$)
γ [2]	0.8	0.018	3.40[3]	4.6
α [2]	1.17	0.077	3.73[3]	22
$\gamma \rightarrow \alpha$ [4]	0.65	0.039	3.59[5]	9.7

1: Specific Heat (Ref. 17) 0.75 $J\ g^{-1}\ K^{-1}$.
2: As-sprayed coating.
3: Mass of sample divided by its volume including open porosity (determined from dilatometry measurements).
4: Heat treated with the torch as in Section 2.6
5: Mass of sample divided by its volume including open porosity (by water immersion).

3. DISCUSSION

For the same torch parameters, a reduction in both the speed that the torch traversed across the substrate and the cooling air pressure had a dramatic effect on the type of Al_2O_3 crystalline phase(s) formed and the microstructure of the coatings.

A fast traversal of the torch across the substrate surface combined with a good flow of cooling air onto the back face of the substrate, enabled fast extraction of heat from the coating. "Conventional" coatings were formed where their crystal structure was composed almost entirely of the metastable phase γ-Al_2O_3 and the coatings had a well defined lamellae structure. It has been calculated[12] that the degree of undercooling required to nucleate the metastable phase, γ-Al_2O_3, in preference to the stable phase, α-Al_2O_3, needs to be of the order of 0.2Tm, ie below approximately 1740°C, although there is considerable uncertainty in this value[9]. This level of undercooling has been recorded in splat quenched metals and those conditions are believed to be similar to those during plasma spraying[9]. The γ-Al_2O_3 crystals would then nucleate homogeneously and grow rapidly into the undercooled melt. As they grow the heat of fusion is liberated and if the heat removal is comparable to, or less than the rate of heat generation, a columnar microstructure results[9] as seen within these lamellae. The grains did not extend from one lamellae to the next, which is indicative that solidification was completed before the next droplet impacted.

From McPherson's[9] estimated temperature-time relationships for Al_2O_3 lamellae as a function of individual lamellae thickness on a substrate at 100°C, solidification after impact of particles to give a lamellae thickness ranging between 1 to 5μm is seen to be completed in less than approximately 10^{-3} sec. The response time needed to achieve this resolution of time was not possible during the temperature measurements of this work because of the combination of the limited response time of the chart recorder and the large thermal mass of the thermocouple junction relative to that of each droplet. However, the temperatures recorded are believed to be an indication of the temperatures experienced by the bulk coating after solidification and it was seen from the temperature profiles that the coating cooled very quickly to between 100 to 200°C in several seconds.

In contrast, when the torch was slowly traversed over a substrate with little or no air cooling, thick coatings containing α-Al_2O_3 were produced. The droplets were well melted and contained no seed nuclei remaining from unmelted powder particles, which means that the α-Al_2O_3 could only have nucleated after impact with the substrate. Since each pass of the torch contained microstructures that could be divided into three types; namely, lamellae with lenticular-shaped pores between them, banded-lamellae and long grains, it is suggested that within each pass the droplets, after impacting the substrate, encountered either one of three different generalised cooling conditions, and these cooling conditions dictated the resultant structure. Fig. 14 is a sketch of each representative microstructure whose mechanism of formation is discussed as follows.

The first droplets to arrive impacted the surface of the previously deposited pass which had cooled to approximately 900°C. Independent lamellae were present, suggesting that, as in the γ-Al_2O_3 coatings, solidification was completed before the next droplet arrived. The lenticular-shaped cracks between the lamellae could arise if the lamellae solidified as γ-Al_2O_3, and then transformed to α-Al_2O_3 from the heat of the torch, since the bulk temperature of the coating rose to over 1300°C. On crystal transformation, the density increased, and so to accommodate the volume decrease, the pores opened between the lamellae and the lamellae cracked. This was referred to as "excessive fragmentation" by Hurley and Gac[5] and was designated Type I microstructure in this study. Sintering should help to close the pores, but it appears to been negligable since the fine grains within the lamellae were easily discerned and there was little grain growth.

An increase in the temperature of the coating, from both the heat of the torch and the heat transferred from the impacting droplets, would reduce the degree of undercooling until it would be energerically favourable

for α-Al_2O_3 to nucleate from the melt in preference to γ-Al_2O_3. If solidification of each lamellae is finished before the next droplet arrives, this could give the banded-lamellae structure, Type II, where the lamellae are still individual, but there is no cracking between them because there is no subsequent transformation. The grain size within these bands is much coarser suggesting that the nucleation events were very limited because of the low level of undercooling. Liberation of the heat of fusion during solidification would result in an increase in the the temperture of the liquid and so suppress the amount of nuclei[9].

As the temperature further increased, a critical point must have been reached when the preceeding droplet has not completely solidified before the next one impacted. Then the top of each lamella would contain a small amount of liquid located between the cellular dendrites tips, as sketched in Fig. 15, and the next droplet thus feeds these growing dendrites so that they could continue to grow without terminating to produce long grains, Type III. The dendrite tips were probably rather fragile so that the force of the next impacting droplet was enough to disturb them and give the wrinkled structure within the columnar grains. Even the long grains in the upper part of that region were wrinkled, so it is likely that the layer of liquid remained thin, even though the substrate continued to increase in temperature. This is furthur supported by the fact that in some places the liquid appeared to have been exhausted during solidification to reveal the dendrite tips, Fig. 7(h). The variation in structure of adjacent regions as seen in Fig. 7(e), may have to do with very slight temperature differences[9].

The torch then moved away from the region of interest, the coating cooled and the top lamellae solidified completely. The coating cooled further so that when the torch returned, the first droplets of the next pass nucleated as γ-Al_2O_3 to give Type I structure.

This three stage type of structure for α-Al_2O_3 was not observed by Huffadine and Thomas[13] because they kept their substrate above 1400°C thus encouraging only Type III crystal growth. They quoted lengths of 12μm, but their micrographs at a magnification of 250 times indicated that some grains were of the order 100μm. The length of the long grains in this work depended on their position within the coating, as those far from the coating centreline were much shorter, as expected since these regions did not receive the full heat of the torch. Fielder[14] also observed both Type I and Type III structures with an apparently abrupt change from one to the other. Since the torch was held stationary, the coating would increase in temperature until it would become energetically favourable for α-Al_2O_3 to nucleate in preference to γ-Al_2O_3.

For the superheated coatings, the liquid pool would be expected to be much deeper and therefore the growing dendrite tips to be more deeply submerged in the liquid, when the next droplet impacts. This could then explain why these grains do not have a wrinkled structure, since they are not effected by the next impacting droplet.

Comparison of X-ray diffraction spectra obtained after progressive heat treatments, Fig. 4, with those obtained after reducing the torch-to-substrate distance, Fig. 3, show that the γ (400) peak can be of the same broad profile yet there is no α-Al_2O_3 in the former. The α-Al_2O_3 in the latter probably arises from unmelted particles being incorporated in the coating because the torch was too close to the substrate for proper melting of the particles. The nomenclature δ'' was used in Fig. 4 to describe the tetragonal phase formed intermediate between the two JCPDS standard cubic and standard tetragonal structures. This should help reduce any confusion which arises when double peaks with non-standard lattice parameters are observed.

X-ray diffraction showed that the steep sides of the thick as-sprayed α-Al_2O_3 coatings contained δ'' - in addition to α-Al_2O_3. It is likely that those droplets that had spread out smoothly and had good contact with the hot coating nucleated directly as α-Al_2O_3, and the parts of those that had splashed and broken up, experienced a greater undercooling, nucleated as γ- Al_2O_3, and subsequently transformed by the heat of the underlying coating and the torch to δ'' -Al_2O_3. If there were facilities to traverse the torch on the vertical axis, as well as the horizontal axis, a flat coating, with particle impact at right angles to its surface, could have been produced and it is anticipated that the amount of the δ'' - phase would be negligable.

The minor broadening of the γ (400) peak on the faces of γ-Al_2O_3 coatings where spraying continued for up to 7 minutes is consistent with the coating having experienced temperatures below 700°C, as seen from the heat treatments, and measured with the thermocouples during spraying.

In porosimetry measurements, in actual fact, the diameter of the channels between the pores is being measured rather than the diameter of the pores themselves[18]. If it is assumed that the connecting channels are of the same size as the pores, it is seen that in the as-sprayed γ-Al_2O_3 coatings there are either many pores around 0.1 μm diameter or there are many large areas around this size to be filled. This assumption is supported by the work of McPherson and Shafer[19] who determined by electron microscopy that there are gaps of order 0.01-0.1μm between the lamellae. Extending this to the as-sprayed α-Al_2O_3 coatings, the wider distribution of diameters would indicate that there are larger pores or cracks present, probably arising from the Type I structure, which had undergone the crack associated γ- to α-

transformation. The number of pores, or cumulative pore volume, is less than the as-sprayed γ-Al_2O_3 coatings because the Type I structure only takes up part of the total structure.

The volume shrinkage of the as-sprayed γ-Al_2O_3, calculated from the linear shrinkage curves, is 0.06%. That due to the crystal transformation is also of this order. Since the coatings are cracked, and therefore the cracks open up, thereby reducing the apparent shrinkage, there may also be a small amount of sintering, with very little, if any, grain growth occurring. The higher thermal expansion coefficent in the direction across the coating thickness, as compared with that along the coating plane for the γ-Al_2O_3 coatings would be expected to be a function of the crystallographic orientation, as the lamellae are composed of short columnar grains growing in the vertical direction. However, for the as-sprayed α-Al_2O_3 coatings, which contained a large columnar grained region, there was very little difference in the two directions. That means that perhaps the difference is due to how the elongated pores between the lamellae opened and closed during heating and cooling, which in turn is related to the area of lamellae-lamellae contact. Lamellae-lamellae contact has been determined to be around 30%[19,20]. The as-sprayed γ-Al_2O_3 coating would be much more sensitive to this as it completely transforms to α-Al_2O_3 during the heating cycle imposed by the dilatometer. The thermal hystresis seen in both coatings, if the shrinkage due to the phase transformation is ignored in the original as-sprayed sample, may also be due to the coatings' internal cracking[21].

The thermal diffusivity of the samples increased in the order: as-sprayed γ-Al_2O_3, as-sprayed γ-Al_2O_3 heat treated by the torch and converted to α-Al_2O_3, and as-sprayed α-Al_2O_3 (which had contained a small amount of γ in each layer before transformation to α). The value of the last mentioned was the same as that of sintered α-Al_2O_3[18]. As expected for the α-Al_2O_3 coatings, that which had transformed from γ-Al_2O_3 would have a lower diffusivity because there is a large amount of cracking and limited contact between the lamellae[22]. The difference between as-sprayed α and as-sprayed γ may be both a consequence of the pore geometry difference and size[23] and the crystal structure. The thermal diffusivity of dense γ-Al_2O_3 is not known since it cannot be fabricated.

4. CONCLUSIONS

Coatings containing >99% γ-Al_2O_3 can be produced when the spraying parameters are optimised. The particles after impact with the substrate spread out on the substrate and nucleated as γ-Al_2O_3, a metastable phase, in preference to the stable phase α-Al_2O_3, and the solidification of each was

finished before the next particle arrived. The heat extraction rates were sufficient to maintain this phase to room temperature.

Particles that had the same in-flight thermal history, but impacted and spread on a substrate that was not air-cooled and so was at higher temperatures, cooled at a far slower rate. This produced three different microstructure types within each pass of the torch, each microstructure occurring at successively higher temperatures.

Type I, in the lower region of each pass, contained a limited lamellae structure with lenticular-shaped pores between the lamellae and the lamellae were cracked. It was believed to form because the impacting particles solidified as γ-Al_2O_3, and solidification was complete before the next droplet arrived, but transformed to α-Al_2O_3 from the heat of the torch as further particles were deposited.

Type II, above Type I, where the structure was termed banded-lamellae and where the particles were believed to have nucleated directly from the melt as α-Al_2O_3. Solidification was complete before the next droplet arrived, so that the lamellae were of regular thickness.

Type III, in the upper region of each pass, which consisted of long grains, in some areas over 200μm in length. Here, grains were believed to have nucleated as α-Al_2O_3 and solidification was not completed before the next droplet impacted. The latter then provided extra liquid to enable continued grain growth and produce the long columar structure.

The structures in this work clearly demonstrated the possible phase changes that can occur during the spraying of α-Al_2O_3 coatings. Should stable, dense coatings of uniform microstructure be desired for high temperature applications, then during their production, the substrate should be heated to over 1300°C using an external heat source. The higher thermal conductivity of these coatings than the as-sprayed γ-Al_2O_3 coatings may also allow their use in the electronic industry where they can conduct heat away from components and yet act as an electrical insulator.

5. ACKNOWLEDGEMENTS.

The first author wishes to acknowledge support of a fellowship from the Science and Technology Agency (Japan) during the course of this work, the use of the research facilities at the Ship Research Institute, and the encouragement given from the other members of the Plasma Spraying group, namely; Dr. S. Amada, Mr. T. Senda and Miss. C. Iino.

6. REFERENCES.

1 N.N. Ault, J. Am. Ceram. Soc.,40(1957)69.
2 N.N. Ault and L.H. Milligan, Am. Ceram. Soc. Bull.,38(1959)661.
3 V.F. Eichhorn, J. Metzler and W. Eysel, Metalloberflache, 26(1972)212.
4 V.S Thompson and O.J. Whittemore, Am. Ceram. Soc. Bull., 47(1968)637.
5 G.F. Hurley and F.D. Gac, Am. Ceram. Soc. Bull., 58(1979)509.
6 K. Sasazaki, Y. Miyamoto and M. Koizumi, J. Ceram. Soc. of Japan, 95(1987)1175.
7 B.C. Lippens and J.H. de Boer, Acta Cryst., 17(1964)1312.
8 JCPDS - Int. Centre for Diffraction Data, U.S.A., Card no. 10-425.
9 R. McPherson, J. Mater. Sci., 15(1980)3141.
10 R. McPherson, 5th Conference on Aluminium Oxide, Prague, Czechoslavakia, August 1990.
11 L. Gorski, Proc. of 11th Conf. on Appl. Crystallogr.,1984, Vol.2, p. 650.
12 R. McPherson, J. Mater. Sci., 8(1973)851.
13 J.B. Huffadine and A.G. Thomas, Powder Metallurgy, 7(1964)290.
14 H.C. Fielder, in J. Szekely and D. Apelian (ed.), Plasma Processing and Synthesis of Materials, Materials Research Society Symposia Proceedings, Vol. 30, 1984, p.173.
15 JCPDS - Int. Centre for Diffraction Data, U.S.A., Card no. 16-394.
16 J.F. Lancaster, Metallurgy of Welding, George Allen and Unwin, London, 3rd edn., 1980, p. 61.
17 Y.S. Touloukian (ed), Thermophysical Properties of Matter, The TPRC Data Series, IFI Plenum, New York, 1973, Vol. 4, p. 102 (Fe), Vol. 10 p.378 (Al_2O_3)
18 M. Vardelle and J.L. Besson, Ceram. International, 7(1981)48.
19 R. McPherson and B.V. Shafer, Thin Solid Films, 112(1984)89.
20 Y. Arata, A. Ohmori and C-J. Lee, Proc. of ATTAC '88, Osaka, May 1988, High Temperature Society of Japan, p.205.
21 R. Morrell, Handbook of Properties of Technical and Engineering Ceramics, Pt. 1, National Physical Laboratory, London, 1985, pp.79
22 R. McPherson, Thin Solid Films, 112(1984)89.
23 F.R. Charvat and W.D. Kingery, J. Am. Ceram. Soc., 40(1957)201.

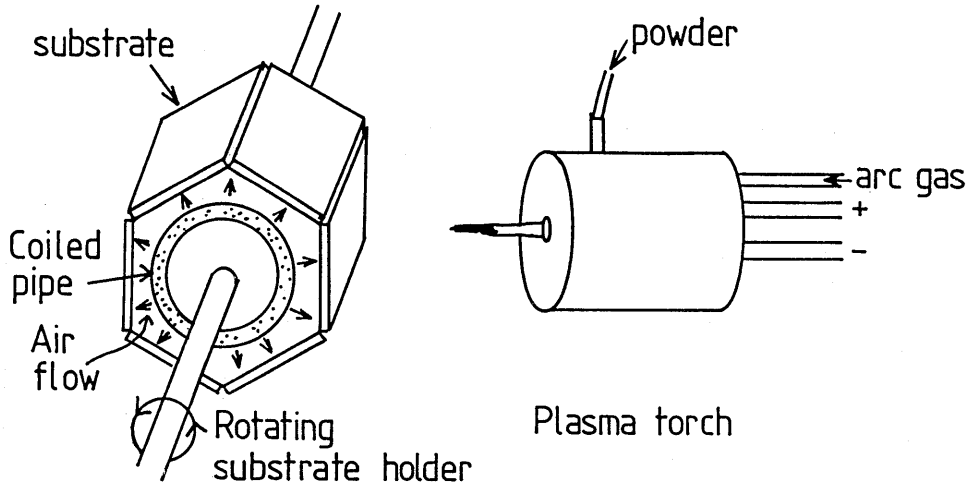

Fig. 1. Experimental arrangement to produce γ-Al_2O_3 coatings.

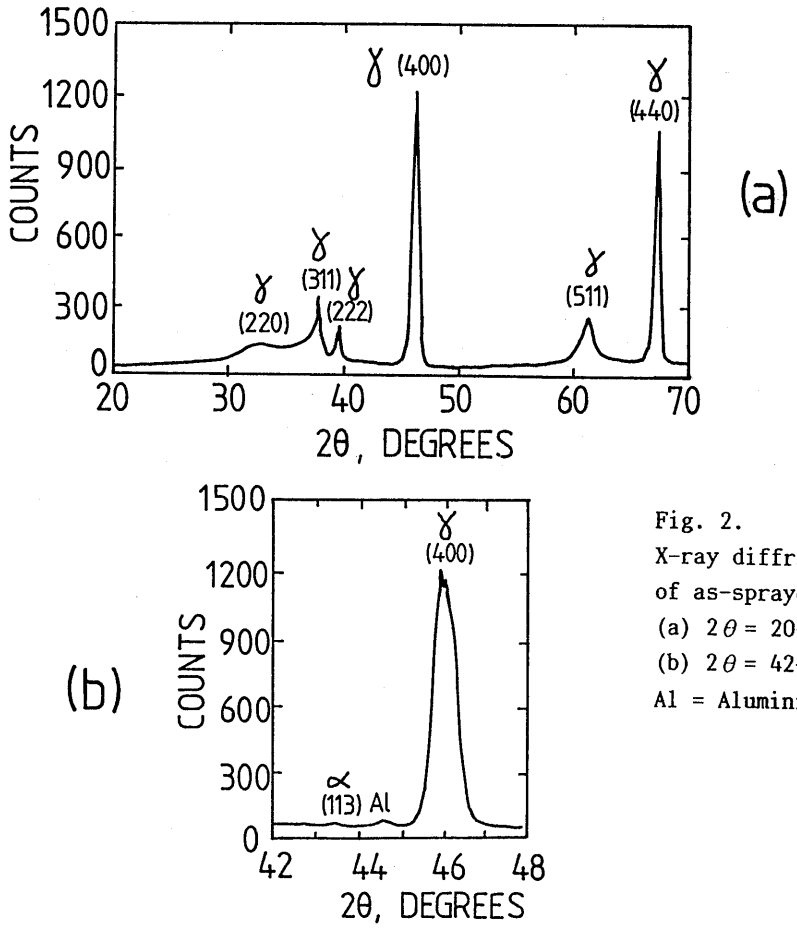

Fig. 2.
X-ray diffraction spectra of as-sprayed γ-Al_2O_3.
(a) 2θ = 20–70°
(b) 2θ = 42–48°.
Al = Aluminium substrate.

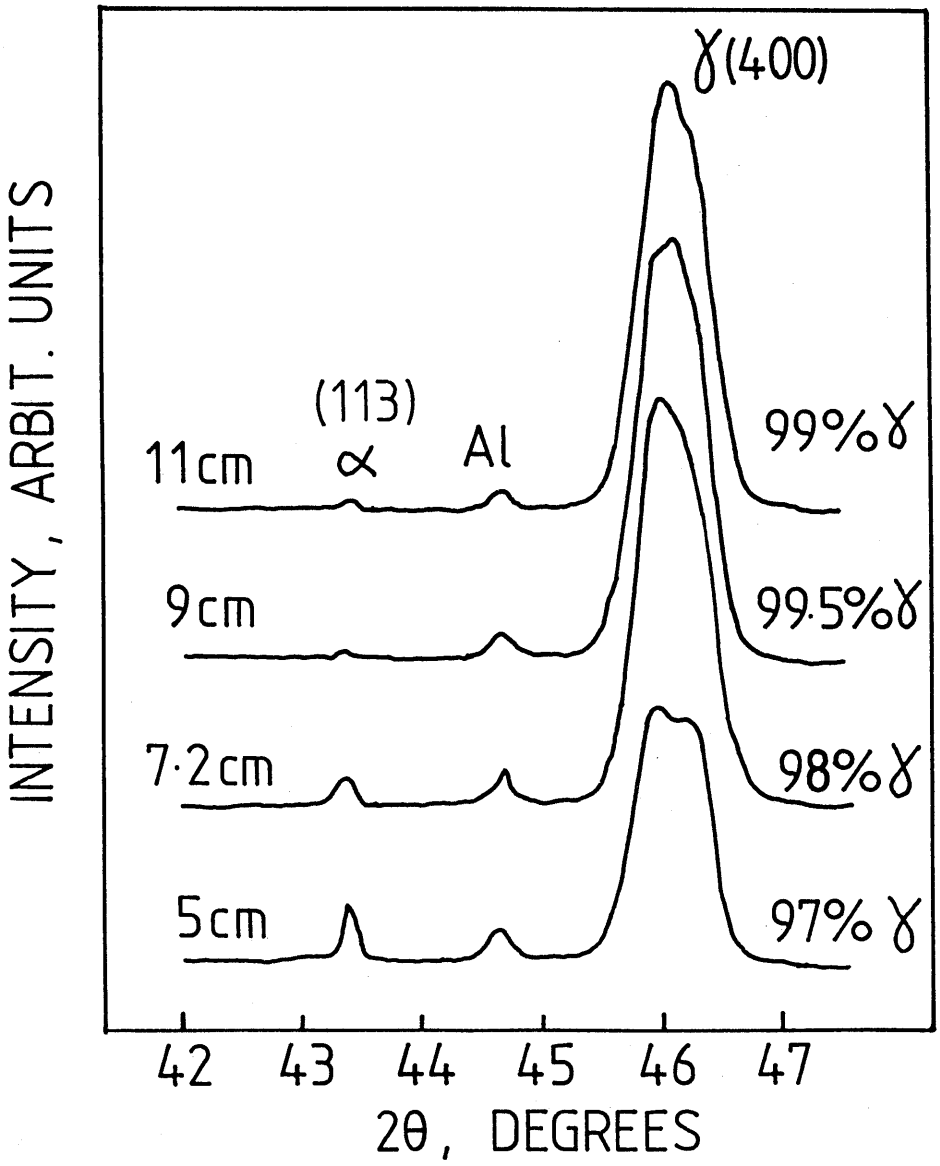

Fig. 3. Change in the proportion of γ-phase and and its (400) peak width versus torch-to-substrate distance.
Al = Aluminium substrate.

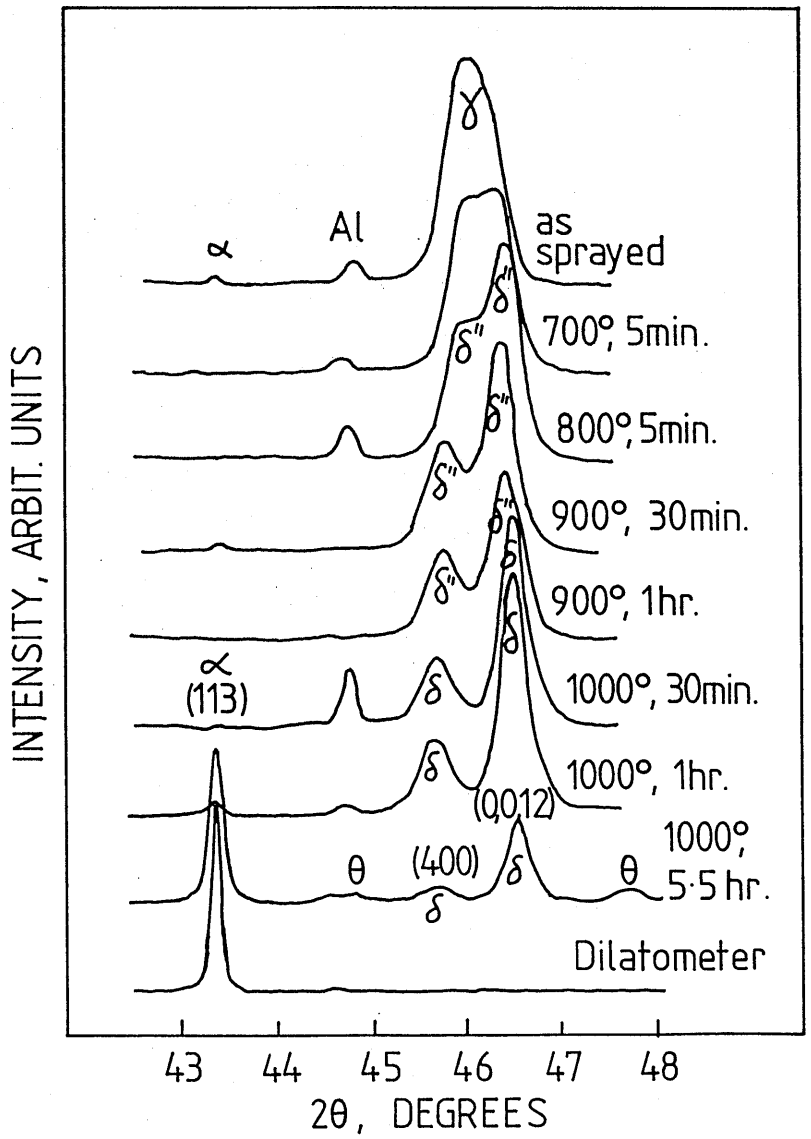

Fig. 4. The effect of heat treatments in air at various temperatures and times on the phase changes in as-sprayed γ-Al_2O_3. The sample placed in the dilatometer was heated at 5°C min^{-1} to 1300°C in argon, and cooled at the same rate. Al = Aluminium substrate.

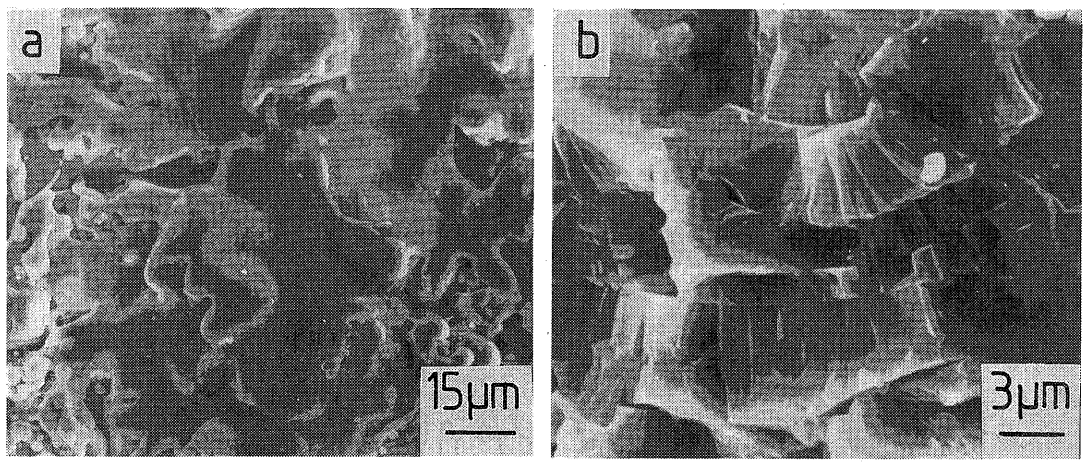

Fig. 5. As-sprayed γ-Al_2O_3 (a) top surface (b) fracture face.

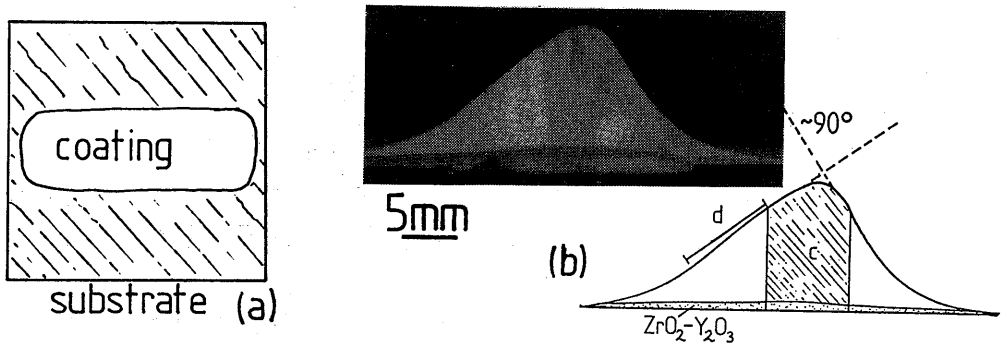

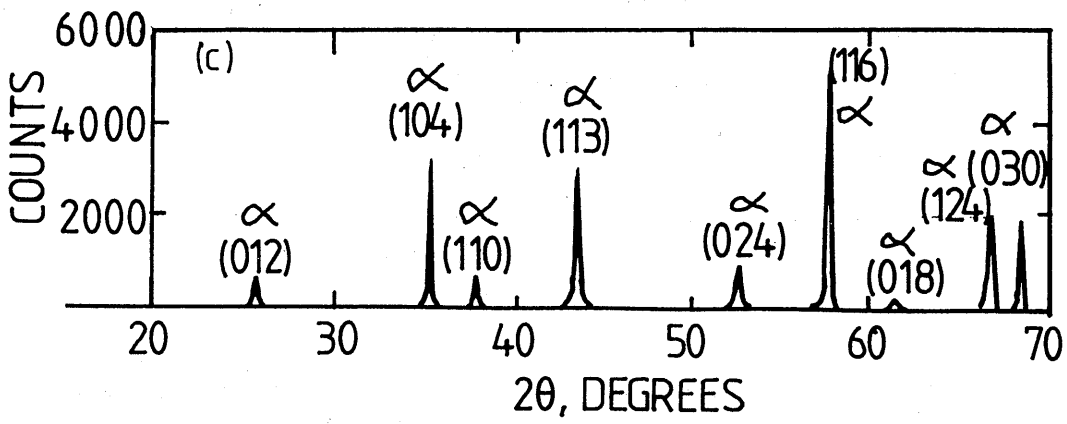

Fig. 6. As-sprayed α-Al_2O_3 coatings (a) schematic top view of coating (b) optical and schematic cross-sectional view (c) X-ray diffraction spectra from central part, crushed

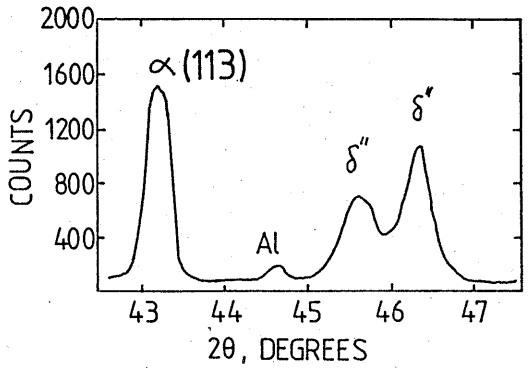

Fig. 6 (cont.)
(d) X-ray diffraction spectra from outer surface down the side.

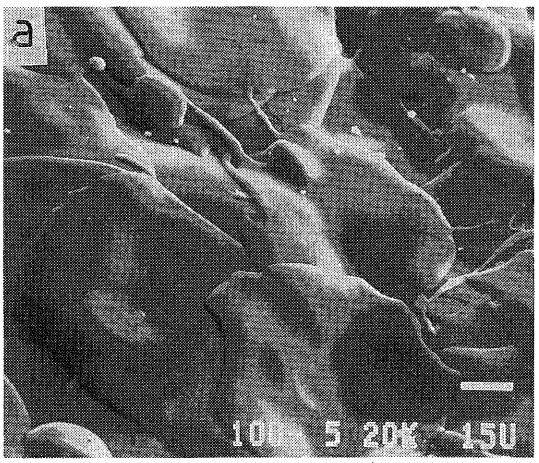

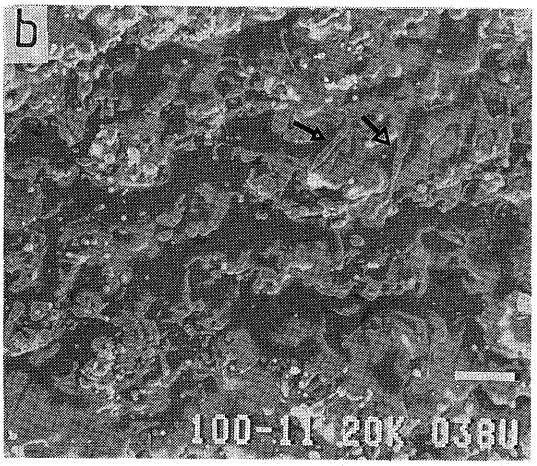

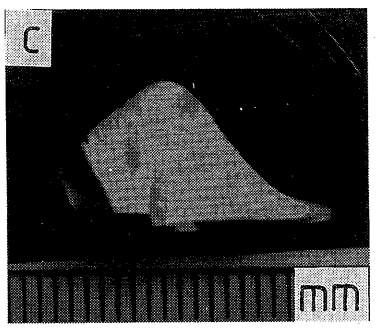

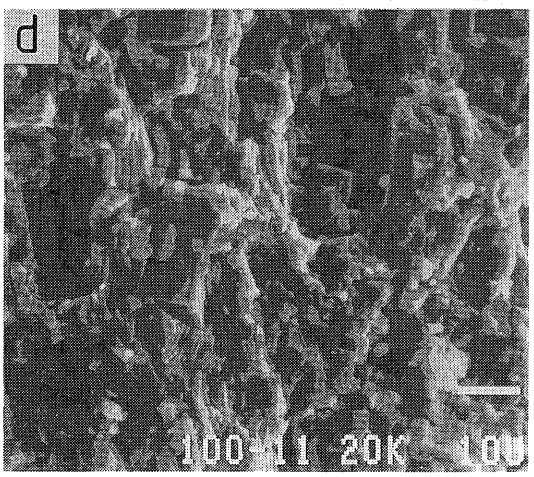

Fig. 7. As-sprayed α-Al_2O_3 (a) top surface of ridge (b) outer surface down the side. "Wet paint drips" morphology arrowed (c) optical cross-section showing a series of bands, one being deposited during each pass of the torch (d) Type I microstructure in lower region of any pass

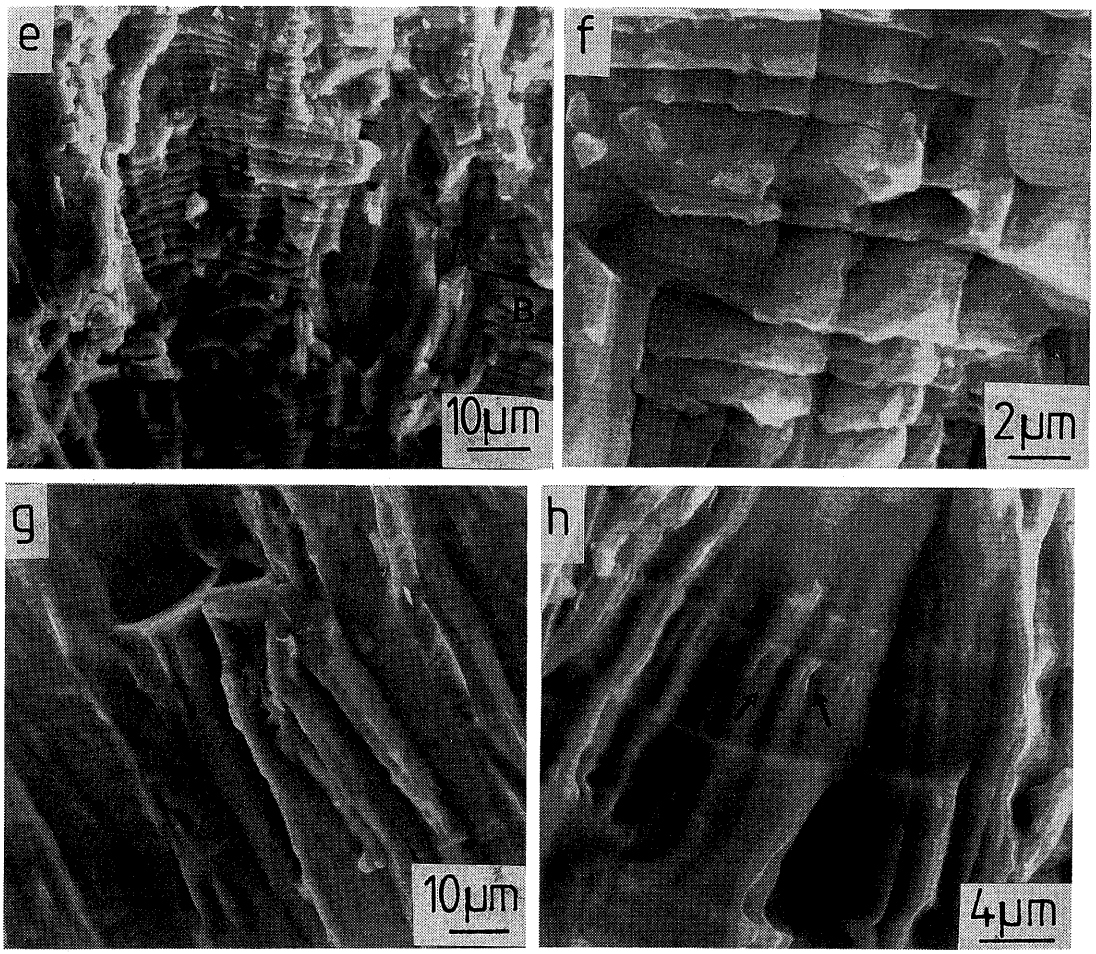

Fig. 7 (cont) (e) second region in pass. Grains become longer, labelled with an "A". Type II microstructure labelled with a "B" (f) higher magnification of Type II microstructure (g) the upper region of any pass showing Type III microstructure which has a wrinkled morphology. Abrupt termination of a grain arrowed. (h) an example of columar grain tips occassionally seen within the Type III microstructure, classified as cellular dendritic (arrowed)

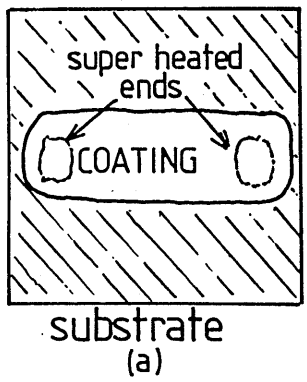

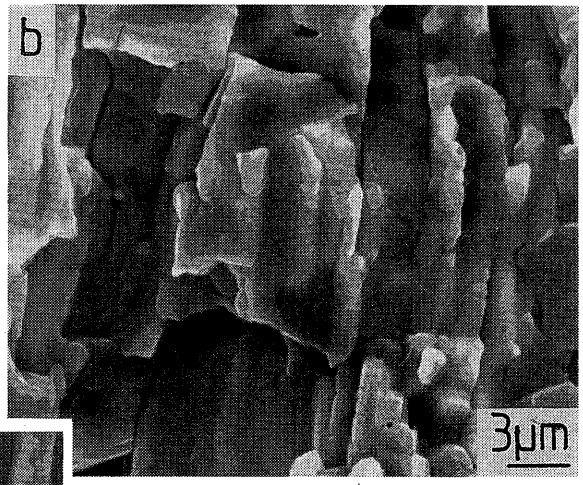

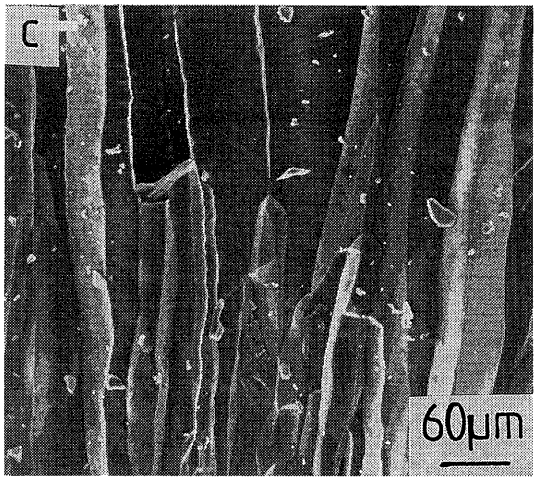

Fig. 8.
Superheated α-Al_2O_3 coating
(a) sketch showing the location of the superheated ends
(b) short grained region showing little sign of the lamellae structure
(c) long grained region

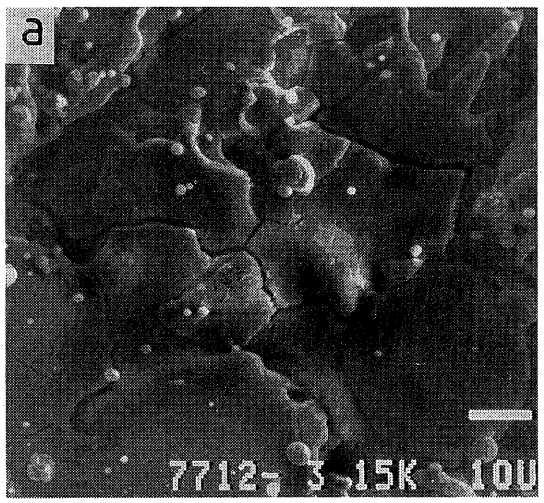

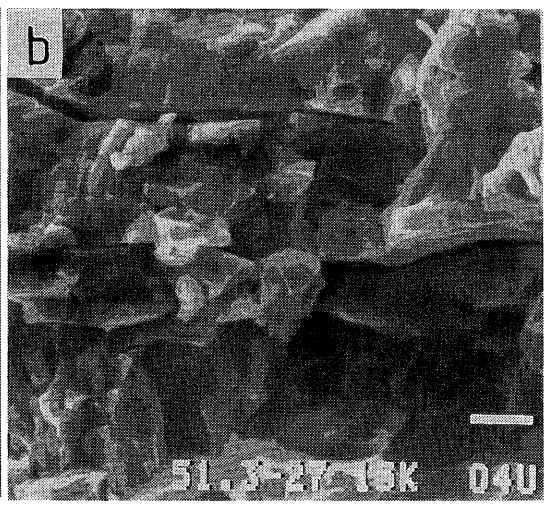

Fig. 9. As-sprayed γ-Al_2O_3 coating heat treated by the plasma torch and converted to α-Al_2O_3. (a) top surface (b) fracture face.

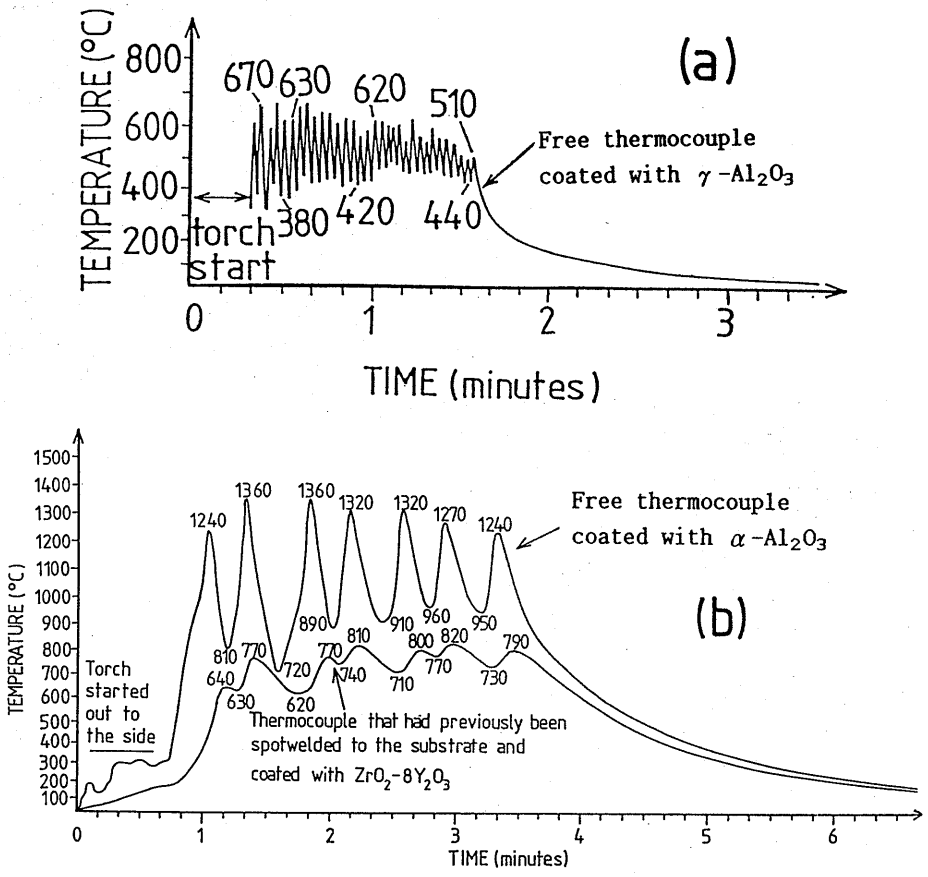

Fig. 10. Temperature profiles measured within the (a) γ-Al_2O_3 (b) α-Al_2O_3 and the ZrO_2-$8Y_2O_3$ coatings during spraying

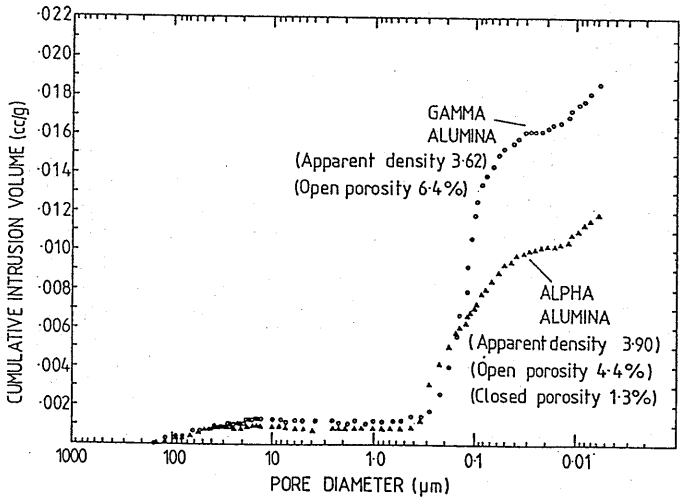

Fig. 11. Cumulative pore size distributions in as-sprayed α- and γ- Al_2O_3 coatings.

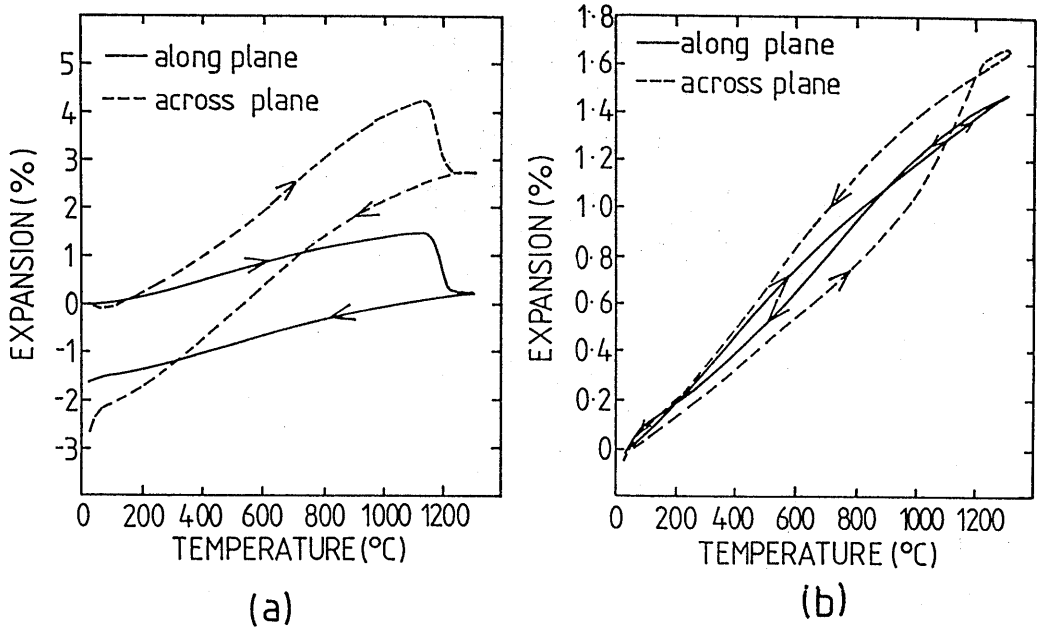

Fig. 12. Thermal expansion curves of (a) γ-Al_2O_3 along and across the plane of the coating (b) α-Al_2O_3 along and across the plane of the coating

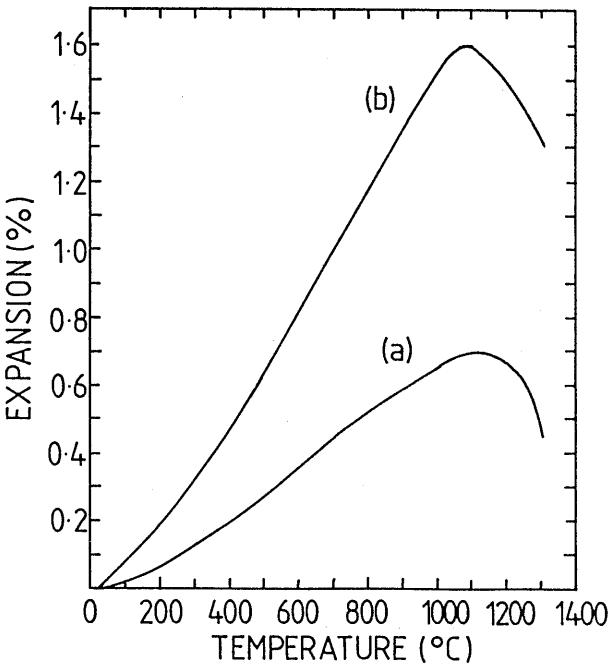

Fig. 13.
Thermal expansion curves of the γ-Al_2O_3 coatings that had been heat treated by the torch and converted to α-Al_2O_3 measured (a) along and (b) across the plane of the coating.

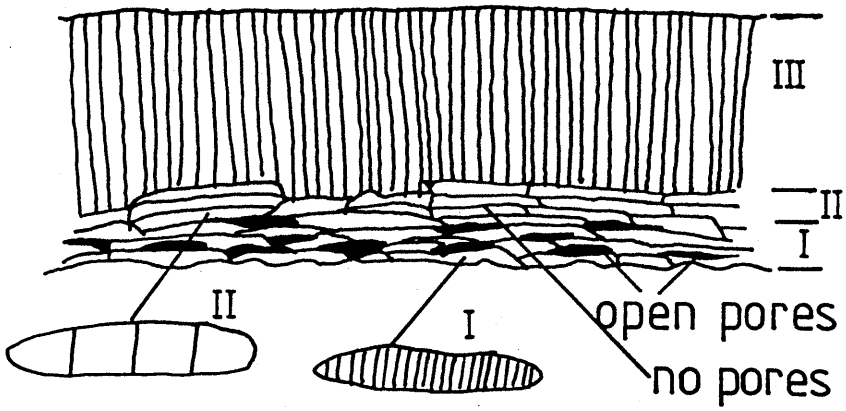

Fig. 14. Schematic summarising the three types of microstructure seen with each pass of the as-sprayed α-Al_2O_3 coatings.

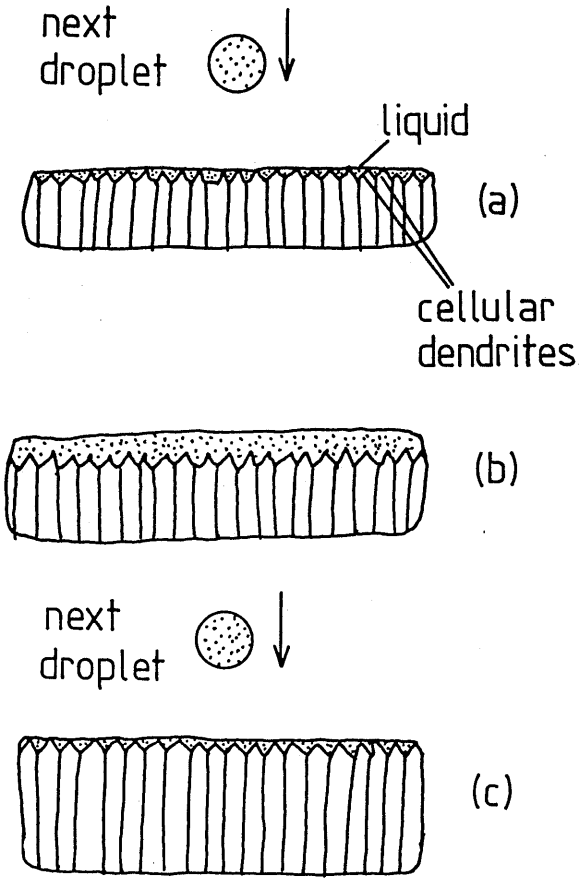

Fig. 15.
Schematic proposing the mechanism of Type III microstructure formation
(a) there is a small amount of liquid remaining between the cellular dendrites as the next droplet advances (b) this droplet impacts and provides extra liquid for dendrite growth (c) the dendrites grow and so the length of the columnar grains increases. The layer of liquid is nearly depleted when the next droplet impacts.